PHYSICAL REVIEW A VOLUME 25, NUMBER 5 MAY 1982

Stationary nonequilibrium states by molecular dynamics. Fourier's law

Alexander Tenenbaum, Giovanni Ciccotti, and Renato Gallico
Istituto di Fisica "G. Marconi," Gruppo Nazionale di Struttura della Materia del CNR, Piazzale Aldo Moro 2, 00185 Roma, Italy

(Received 19 October 1981)

We have developed a technique to produce stationary nonequilibrium states in a molecular-dynamics system; this method is based on the introduction of stochastic boundary conditions to simulate the contact with a thermal wall. The relaxation times involved in such contact are short enough ($\sim 10^{-11}$ sec) to make the technique suitable for computer experiments. The method allows the simulation of bulk properties in a system coupled with a heat reservoir and the study of the local thermodynamical equilibrium. Furthermore, it gives a physical description of the heat transfer near a thermal wall. The method has been applied to simulate high thermal gradients in a region of dense fluids ranging from the gas-liquid coexistence line to the freezing line, to check the validity of the linear thermal response (Fourier's law). We have found that the linear region extends at least up to gradients of the order of 1.8×10^9 K/cm for argon. In the bulk region where boundary effects are negligible we have verified the validity of the local equilibrium hypothesis for all simulated gradients.

I. INTRODUCTION

In a previous paper[1] we presented some results obtained by introducing stochastic boundary conditions in molecular-dynamics (MD) computer experiments. We were able to simulate the contact of a MD system with a thermal reservoir in the dense-fluid region. It has been shown there that this technique can be used to simulate stationary nonequilibrium states. In particular a thermal gradient was obtained by placing the system between two thermal walls at different temperatures. This permitted the study of thermal-transport phenomena. The technique implied the simulation of thermal gradients which are much higher than the experimental ones, to obtain a satisfactory signal-to-noise ratio. However, the computed values of the thermal conductivity were in good agreement with experimental data and consistent with the ones obtained by Ashurst[2] via a different nonequilibrium simulation technique and by Levesque[3] via equilibrium Kubo formulas. This result showed the validity of the Fourier's law in the region of the smallest gradients needed for nonequilibrium MD experiments.

It is now interesting to look for the limits of validity of the Fourier's law, i.e., the possible breakdown in the linearity of the phenomenological law for thermal transport. This can be done by increasing the thermal gradient applied to the system. In this paper we present the results obtained by studying the region of dense fluids. The main conclusion we can draw within the precision of our method is that there is no deviation from linearity for gradients greater than 5×10^7 K/cm and up to 1.8×10^9 K/cm.

In Sec. II, we give details of the model with stochastic boundary conditions. In Sec. III we describe the computer experiments. In Sec. IV we study in detail the thermalization mechanism and the phenomenon of thermal transmission through the thermal wall. In Sec. V we analyze the validity of the local equilibrium hypothesis and present the results obtained for the thermal conductivity in various thermodynamical states. Section VI is devoted to some concluding remarks.

II. THE MODEL

As indicated in Ref. 1, we consider a system of N particles enclosed in a cube Λ of side L, interacting through a two-body potential of the Lennard-Jones type:

$$u(r)=4\epsilon\left[\left[\frac{\sigma}{r}\right]^{12}-\left[\frac{\sigma}{r}\right]^{6}\right]. \tag{1}$$

As usual,[4] we cut the potential at a distance $R_c=3\sigma$; our units are σ for length, ϵ for energy, and $\tau=(m\sigma^2/48\epsilon)^{1/2}$ for time ($\sigma=3.405$ Å, $\epsilon=119.8k_B$, $\tau=3.112\times10^{-13}$ sec for argon).

The boundary conditions are periodic in the directions y,z, while in the x direction Λ is bounded by thermal walls realized in the way described below. Thus, the equations of motion to be integrated are

$$m\frac{d^2\vec{r}_i}{dt^2}=-\sum_{j\neq i}^{1,N}{}_j\vec{\nabla}_{\vec{r}_i}u(r_{ij})+\vec{f}_w(\vec{r}_i)\ ,\quad i=1,N \tag{2}$$

where $\vec{f}_w(\vec{r})$ is an impulsive stochastic force acting on the particle only when the latter strikes a thermal wall. The effect of this force is such that a particle arriving at the wall is reentered into the box at the same place, but with a velocity sampled from the following probability density. In the y and z directions the velocity components of the reentering particle are drawn from a Maxwellian distribution at the wall temperature T; in the x direction the velocity component is sampled from the probability density

$$\phi(v_x)=\frac{m}{k_BT}v_x\exp\left[-\frac{mv_x^2}{2k_BT}\right], \tag{3}$$

where v_x must have the same sign as the x component of the inward normal at the stochastic wall, i.e., $v_x\geq0$ at the left wall and $v_x\leq0$ at the right wall.

Such a simple surface mechanism to realize the contact between a fluid and a heat reservoir has been proposed by Lebowitz and Spohn[5] and used to demonstrate the existence of the Fourier's law in a Lorentz gas. Furthermore, Goldstein *et al.*[6] have established the efficiency of this mechanism to thermalize a model system. In this way a dynamical realization of a canonical ensemble can be obtained. In Ref. 1 it was shown how to implement this mechanism in computer experiments. There we obtained, for systems of some hundred particles in the region of dense fluids, satisfactory results for the thermalization and the energy fluctuations.

The results on the validity of the thermal-contact mechanism have been confirmed for the new thermodynamical states studied in the paper at hand. In particular at the highest density ($\rho=1.113$) the canonical equilibrium temperature in a run of 2000 time steps does not differ by more than 1.3% from the wall temperature. Moreover, the specific heat at constant volume is 2.37 in the canonical case, to be compared with the microcanonical value 2.39. No experimental data are available for this thermodynamical state; however, Levesque[3] has found the value 2.74 for a microcanonical simulation at the same density and temperature. We believe that this discrepancy may be attributed to the poorer statistics of our runs.

The simulation of a thermal wall in our MD experiments has been realized in the following way. The set of coupled differential equations (2) is integrated with the central difference algorithm[4]:

$$\vec{r}_i(t+h)=2\vec{r}_i(t)-\vec{r}_i(t-h)+\frac{\vec{f}_i(t)}{m}h^2\ , \tag{4}$$

where $\vec{r}_i(t)$ is the position of the ith particle at time t, and $\vec{f}_i(t)$ is the first term of the right-hand side in formula (2). The value of the time step in our computations is always $h=0.032$.

The new feature in set (2) is the presence of the stochastic impulsive force $\vec{f}_w$. When a particle j at time t has just crossed a stochastic wall passing during a time step from $\vec{r}_j(t-h)$ to a position $\vec{R}$ at time t, the following procedure is started.

(i) A new velocity $\vec{v}$ is sampled from the described probability density.

(ii) The colliding particle is moved to a new position according to $\vec{r}_j(t)=\vec{R}+\vec{v}h$. [see Fig. 1(a).]

(iii) To use algorithm (4) one updates the position at time $t-h$ as $\vec{r}_j(t-h)=\vec{R}$.

(iv) If $\vec{r}_j(t)$ is still beyond the thermal wall, one substitutes $\vec{r}_j(t)+\vec{a}$ for $\vec{r}_j(t)$ and $\vec{r}_j(t-h)+\vec{a}$ for $\vec{r}_j(t-h)$, where $\vec{a}$ is the difference between $\vec{r}_j(t)$ and its projection on the wall. [Fig. 1(b).]

(v) The positions of the particles which have not crossed a thermal wall are not affected.

(vi) Algorithm (4) is used again for all particles.

We have checked that the slight difference between the ideal mechanism and the numerical implementation does not affect in any appreciable way the final potential energy of the particle, thus preserving the purely kinetic character of the thermalization mechanism.

III. THE COMPUTER EXPERIMENT

The first part of the computer experiment consists in the realization of a chosen thermodynamic

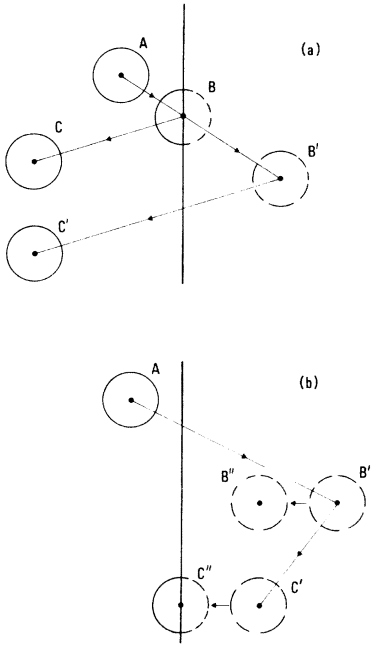

FIG. 1. Reentry mechanism at the thermal wall. (a) A particle in A at time $t-h$ crosses the wall in B in the time interval $(t-h,t)$. The thermalization mechanism would bring it in C at time t. Due to the discreteness of the integration algorithm the particle will be in B' at time t. Therefore the reflection is accomplished by endowing the particle in B' with the thermal velocity and moving it to C' while the other particles are kept fixed. For the numerical algorithm C' is the (new) position at time t, and B' is the (new) position at time $t-h$. (b) If the particle is still beyond the thermal wall after the previous step, it is moved to the wall in C'', while the position B' is moved by the same amount to B''. C'' is the (new) position at time t, and B'' is the (new) position at time $t-h$.

equilibrium state at temperature $T_{\rm eq}$. In this stage the system has the usual periodic boundary conditions[4] and therefore the total energy is conserved. At a given time $t=t^*$ the two boundaries orthogonal to the x axis are transformed into thermal walls, while the other boundaries remain periodic: in this way the translational invariance of the system is kept along y and z directions. Starting from the configuration at t^* the system enters a transient stage; putting the two thermal walls at temperatures T_c (cold wall) and T_h (hot wall) the system relaxes toward a stationary nonequilibrium state characterized by a thermal gradient. To fasten the transient stage, T_c and T_h are such that $(T_c+T_h)/2=T_{\rm eq}$.

Once the transient stage is over, thermodynamic properties can be computed via time averages of suitable microscopic quantities. Because in this model the boundary conditions in the x direction are not periodic, there are no "images" of particles beyond the stochastic walls. Thus surface effects affect some "local" thermodynamic properties (like the density near the wall). Because the size of a typical MD system is small, these effects can become relevant; however, in the study of thermal-transport phenomena it is possible to keep such effects under control, as we shall see later.

The thermodynamic study of the transient and stationary states must be performed from a local point of view to monitor the onset of the thermal gradient. For this purpose the system has been divided into N_L layers of equal size parallel to the stochastic walls, and computing in each layer the smoothed values of the local density, temperature, potential energy, pressure, and heat current. The computation of these values goes as follows. The local value of an observable A at point $\vec{r}$ is

$$A(\vec{r})=\langle A(\vec{r}\,|\,\{\vec{r}_i,\vec{p}_i\}_{i=1,N})\rangle\ , \tag{5}$$

where the quantity to be averaged can in general be written as the sum over the particles of the corresponding property defined for each particle. Thus

$$A(\vec{r}\,|\,\{\vec{r}_i,\vec{p}_i\}_{i=1,N}) = \sum_1^N {}_i A_i(\{\vec{r}_j,\vec{p}_j\}_{j=1,N})\delta(\vec{r}-\vec{r}_i)\ , \tag{6}$$

where A_i is equal to: (i) 1 for the density $\rho(\vec{r})$; (ii) $[3k_B\rho(\vec{r})]^{-1}\,mv_i^2$ for the temperature; (iii) $[2\rho(\vec{r})]^{-1}\sum_{j\neq i}{}_j\,u(r_{ij})$, where $\vec{r}_{ij}=\vec{r}_i-\vec{r}_j$, for the internal energy. For pressure and energy current one has,[7] respectively,

$$A_i=\frac{1}{3}\left[\frac{p_i^2}{2m}-\tfrac{1}{2}\sum_{j\neq i}{}_j r_{ij}u'(r_{ij})\right] \tag{7}$$

and

$$\vec{\mathrm{A}}_i=\left[\left[\frac{p_i^2}{2m}+\tfrac{1}{2}\sum_{j\neq i}{}_j u(r_{ij})\right]\overleftrightarrow{I} -\tfrac{1}{2}\sum_{j\neq i}{}_j\frac{u'(r_{ij})}{r_{ij}}\vec{r}_{ij}\vec{r}_{ij}\right]\cdot\frac{\vec{p}_i}{m}\ . \tag{8}$$

The value of the observables in layer σ $(\sigma=1,N_L)$ is finally

$$A_\sigma(\{\vec{r}_i,\vec{p}_i\}_{i=1,N}) = \frac{1}{V_L(\sigma)}\int_{V_L(\sigma)} d\vec{r}\, A(\vec{r}\,|\,\{\vec{r}_i,\vec{p}_i\}_{i=1,N}) , \quad (9)$$

where V_L is the volume of the layer σ. The smoothed values of the thermodynamic quantities in each layer are then obtained by averaging in time the corresponding observables (9). The thickness l of the layers is determined by a compromise between two opposite requests: (i) the local thermodynamic analysis suggests to use a small V_L; (ii) the number of particles in each layer should be high to improve the statistics of the time averages. In practice a successful compromise has been the following: a cubic system of 256 particles has been divided in 8 layers, each containing an average of 32 particles. This corresponded to choosing the thickness of each layer equal to that of an atomic layer in the solid at the same density.

The computation of the local thermodynamical properties permits to test the validity of the local equilibrium hypothesis. A weak form of the latter is the following: in a stationary state a thermodynamical property Φ depends on the position only through the independent thermodynamical variables $X(\vec{r})$, $Y(\vec{r})$, i.e.,

$$\Phi(\vec{r})=\Phi(X(\vec{r}),Y(\vec{r})) .$$

In the present computer experiments the pressure P should be constant in the system due to the absence of mass current, while density ρ and temperature T vary from layer to layer. Therefore we compared the density values given by the experimental equation of state $\rho_{\text{expt}}=\rho(T(\vec{r}),P)$ with the values computed for $\rho(\vec{r})$. The results confirm the validity of the weak local equilibrium hypothesis and are discussed in Sec. V.

In the transient stage the local values of thermodynamic quantities are time dependent. This time evolution can be observed by taking averages over short time intervals (typically 250 steps). As one can expect these short averages fluctuate strongly. Nevertheless, a definite trend can be observed in the transient stage. For example, looking at the time evolution of the local temperatures of the layers near the thermal walls, one observes that these quantities first drift in opposite directions and then start fluctuating around a stationary value after a short time (typically 500—1000 time steps; see Fig. 2). In our runs we choose to start the evaluation of the stationary averages after a time interval of 2000—4000 time steps, to be sure that the transient stage was over. Furthermore, the thermal gradient was checked during the stationary stage and showed fluctuations but no drift, thus indicating that the system had reached a satisfactory stability.

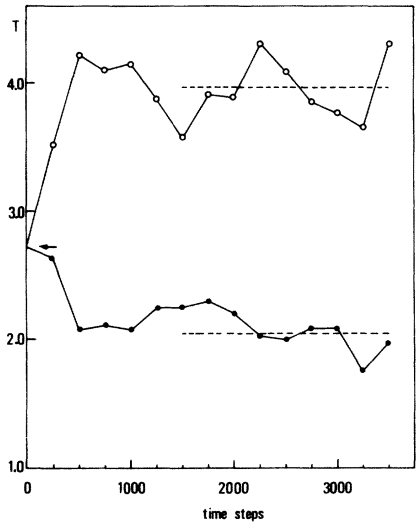

FIG. 2. Time evolution of the local temperature near the thermal wall during the onset of a thermal gradient. Each value is a time average over 250 steps. ● (○) temperature of the layer second nearest to the cold (hot) wall. The arrow indicates the average initial temperature. The dashed lines indicate the final averaged values of the two local temperatures (the averages initiate after 1500 steps). The density of the system is $\rho=1.113$.

IV. THERMAL STATIONARY STATES

The procedure for setting up a thermal gradient initiates from an equilibrium state at given density and temperature.

The thermodynamical states chosen as starting points for setting up the thermal gradients, given in Table I, are in the region of dense fluids.

The systems used for the computer experiments

TABLE I. List of initial thermodynamical states. ρ is the number density, T is the temperature, and P is the pressure (reduced units). n is the number of different gradients realized in the given state.

ρ	T	P	n
0.75	0.909—1.296		5
0.85	0.801	0.5	5
1.113	2.720	22	4

were cubic with 256 particles, except one case with $N=864$; in that case the system was parallelepiped and the distance between thermal walls was the same as in the cases with lower N. The point $\rho=0.75$, $T=0.909$ lies near the gas-liquid coexistence line and the point at $\rho=1.113$ is near the freezing line. Usually different gradients have been realized starting from the same thermodynamical state; at $\rho=0.75$ we started from three different temperatures.

At the end of the transient stage the system exhibits a thermal gradient, which is generally lower than the gradient imposed by the boundary conditions. Almost all gradients show the same feature: the temperature profile in the six internal layers is fairly linear, but with a slope lower than the one of the imposed gradient (Fig. 3). Furthermore, the center of the temperature profile obtained by linear least-squares fit through the six internal layers is often at a different temperature than the center of the imposed gradient, usually lower; let δT be this difference. The temperatures of the outermost layers (T_1, T_8) lie usually between the corresponding wall temperature (T_c, T_h) and the temperatures obtained at the walls by extrapolating the internal temperature profile (T_c', T_h'). Thus the result of the simulation is characterized by the parameter $\tan\alpha$ which determines the obtained gradient, and by the temperature differences δT, $\Delta T_c = T_c' - T_c$, and $\Delta T_h = T_h - T_h'$ which relate this gradient to the imposed one.

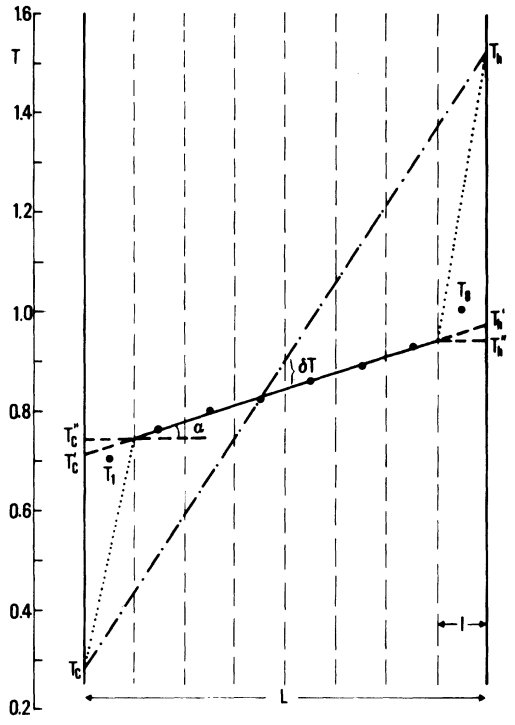

FIG. 3. Imposed and obtained thermal gradient. L is the distance between thermal walls, l is the thickness of an atomic layer. T_c (T_h) is the temperature of the cold (hot) wall; the dots indicate the local temperatures T_1 through T_8. — · — · —: applied gradient. —: gradient obtained by linear least-squares fit through the six internal layers. · · · · : local gradients across the outermost layers. δT is the difference between the temperatures at the center of the applied and obtained gradients. The figure refers to a case at density $\rho=0.75$.

An insight into this behavior can be gained by studying the temperature jumps at the walls $(\Delta T_c, \Delta T_h)$ as a function of the applied gradient at $\rho=0.75$ and 0.85 (Fig. 4). ΔT_c and ΔT_h increase roughly linearly with the temperature difference between the thermal walls for gradient up to 0.2; ΔT_h is always greater than ΔT_c for a given gradient, and there is no appreciable difference between the behavior at $\rho=0.75$ and that at $\rho=0.85$.

For gradients higher than 0.2, ΔT_c continues its linear increase with ∇T, while ΔT_h increases more rapidly, as stressed by the broken line in Fig. 4.

At the density $\rho=1.113$ the temperature jumps at the walls are much lower (at equal applied gradient) than in the previous cases. The higher efficiency of the thermalization mechanism is clearly related to the higher density. Indeed the number of collisions between particles and thermal walls, normalized per unit time and unit area of the thermal wall, is about an order of magnitude greater at this density.

The temperature jump that we observe between the thermal wall and the adjacent fluid is a phenomenon which is well known as an error source

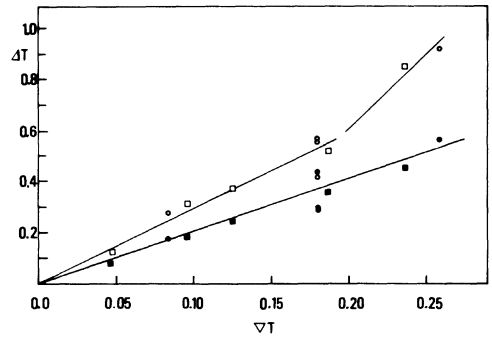

FIG. 4. Temperature jump ΔT at the thermal wall as a function of the applied gradient ∇T. $\rho=0.75$: (●) ΔT_c, (○) ΔT_h. $\rho=0.85$: (■) ΔT_c, (□) ΔT_h.

in experiments performed to measure the thermal conductivity of fluids.[8] The relation between the temperature jump ΔT_α ($\alpha=c,h$) and the gradient *at the wall* is usually given as

$$\Delta T_\alpha = w \mid \vec{\nabla} T_\alpha \mid / P \ , \tag{10}$$

where P is the pressure in the fluid and w is a factor which depends on the state of the fluid and on the nature of the thermal wall. The usefulness of formula (10) is due to the fact that the proportionality factor w should vary slowly with the thermodynamical state of the fluid.

Formula (10) applies when the fluid is a gas and accounts for the temperature jump which extends over a region comparable with the mean-free path of the molecules. In our computer experiments the fluid is dense and the very concept of mean-free path is of course questionable. Nevertheless it may be assumed that, for the effect under investigation here, an effective mean-free path may be defined which corresponds approximately to the thickness of an atomic layer. And indeed we find that the region near the thermal walls, where a temperature jump exists, has an extension of the order of one of the layers defined in Sec. III.

The local gradient which appears in formula (10) has therefore been computed as $(T_c'' - T_c)/l$ near the cold wall and $(T_h - T_h'')/l$ near the hot wall, where T_c'' and T_h'' are the temperatures at the borders of the region in which the temperature profile is almost linear (see Fig. 3).

Assuming the validity of formula (10) one can calculate w in the various simulated states for both the hot and the cold wall. What one finds is that w depends very strongly on the pressure; moreover, in some cases P is even negative. This is not an inconsistency of relation (10) because it is usually employed for diluted gas, while we are in the region of dense fluids. This fact suggests an alternative description of the phenomenon of the temperature jump: the latter may be related to the local gradient $\vec{\nabla} T_\alpha$ via the formula

$$\Delta T_\alpha = w' \mid \vec{\nabla} T_\alpha \mid / \rho_\alpha T_\alpha \ , \quad \alpha=c,h \tag{11}$$

where ρ_α and T_α are the local density and local temperature in the layer across which the local gradient $\vec{\nabla} T_\alpha$ is measured. If one assumes the validity of local equilibrium, the substitution of P by $\rho_\alpha T_\alpha$ in a diluted gas is permitted, and formula (11) follows.

In the case of dense fluids relations (10) and (11) are of course not equivalent, but the latter is well defined for all thermodynamical states. Therefore we chose relation (11) in which w' is assumed to vary slowly with the state of the fluid.

In Fig. 5 the values of ΔT_α are reported as a function of $\mid \vec{\nabla} T_\alpha \mid / \rho_\alpha T_\alpha$ for all gradients. As expected the pattern of the reported points gives for w' definite values, varying from about 0.75 near the origin to about 0.30 when $\mid \vec{\nabla} T_\alpha \mid / \rho_\alpha T_\alpha$ exceeds 3. In the figure the two points marked by an arrow are clearly outside the linear pattern. These points correspond to the hot wall of the two highest gradients simulated and seem to indicate that for very high temperatures and/or gradients the thermal contact between thermal wall and fluid partially breaks down. A similar effect has already been observed in Fig. 4 for the lower densities.

V. RESULTS

A. Local thermodynamical equilibrium

We have performed a local thermodynamical analysis of the simulated stationary states to check the validity of the weak local equilibrium hypothesis mentioned at the end of Sec. III. For this purpose we have compared the layer density ρ_σ ($\sigma=1,8$) with experimental value[9] $\rho_{\text{expt}}=\rho(T_\sigma,P)$.

We report in Table II the results for the most critical case, that is the highest gradient, at $\rho=0.85$. The value for the pressure has been obtained by averaging the values of the six internal layers computed by (7) and (9). The local pressure values of the two outermost layers have been ex-

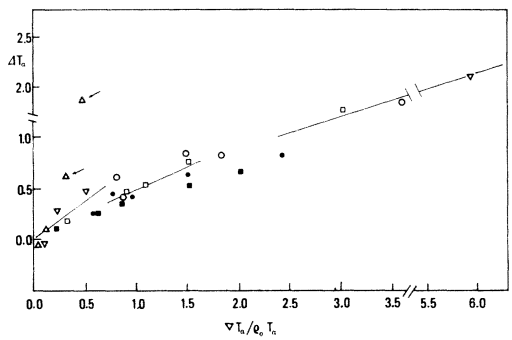

FIG. 5. Temperature jump ΔT_α at the thermal wall as a function of the variable $\nabla T_\alpha/\rho_\alpha T_\alpha$ where ∇T_α is the local gradient, ρ_α the local density and T_α the local temperature near the wall. The slope of the straight segments is the coefficient w'. Symbols as in Fig. 4. $\rho=1.113$: (∇) cold wall, ($\triangle$) hot wall. The arrows refer to the text.

TABLE II. Local equilibrium test. T_σ and ρ_σ are, respectively, the local temperature and density. ρ_{expt} is the interpolated and/or extrapolated experimental datum from Ref. 9 corresponding to T_σ, P. Δ is the percental difference between the computed and the experimental density. Average density $\rho=0.85$. Average temperature $T=0.801$. The pressure in the system is $P=0.50$.

Layer	T_σ	ρ_σ	ρ_{expt}	$\Delta(\%)$
1	0.514	0.927	0.942	−1.6
2	0.592	0.915	0.913	0.2
3	0.649	0.902	0.891	1.2
4	0.706	0.863	0.870	−0.8
5	0.764	0.845	0.848	−0.4
6	0.806	0.839	0.832	0.8
7	0.819	0.806	0.827	−2.6
8	0.946	0.704	0.768	−8.3

cluded from the average because they lie systematically outside the range of the internal values. The reason for this is that forumula (7) is valid in the bulk and does not apply near the walls, where the force field on the particles is altered by the absence of "images" beyond the wall. This effect, however, affects only the outermost layers; therefore the bulk value of the pressure must be computed from the remaining six internal layers.

The agreement found between the experimental and computed values of the density is quite satisfactory and makes one confident in the weak local equilibrium hypothesis. The only relevant deviation is found for layer 8, the one at the highest temperature. This deviation must be ascribed to the lack of images which affects quantities like local density, internal energy, and pressure, but is essentially irrelevant for kinetic quantities. This can be seen in the canonical equilibrium state, where the kinetic energy is uniform through the system while the local values of the other mentioned quantities in the boundary layers deviate from the bulk values. What essentially happens is that the density of the boundary layers is increased or decreased with respect to the average value depending on the compressibility factor $P/k_B\rho T$ being greater or smaller than 1. Thus at $\rho=0.85$, $T=0.801$, and $P=0.5$ we find that the density of the outermost layers is lowered at equilibrium. In the stationary gradient states the sign and the magnitude of this effect may be different at the two walls. In particular for the case reported in Table II we find a significant decrease in ρ only near the hot wall.

A comparison with experimental data is not possible in the region $\rho\simeq1.113$, $P\simeq22$ because no such data are available. Nevertheless a comparison can be done with the equation of state obtained with the perturbation theory of Verlet and Weis.[10] The result seems to confirm the validity of the weak local equilibrium hypothesis only for the central region of the system, while the surface effect on density extends here over at least two layers near each wall. The fact that the compressibility factor is of the order of 7 explains the enhancement (up to 20%) of the boundary density. Here too, however, the kinetic properties do not seem to be affected by the lack of images.

B. Fourier's law and thermal conductivity

In Sec. IV it has been shown that all simulated stationary states exhibit a fairly linear temperature profile through the six internal layers, while the temperatures of the two boundary layers lie often outside that profile due to the thermal transmission near the thermal walls. It is, therefore, convenient to define the resulting thermal gradient $\vec{\nabla}T$ via the linear regression through the temperature values of the six inner layers. The corresponding energy current $\vec{J}^E$ parallel to the gradient has been calculated by formulas (6), (8), and (9), with the further average $\vec{J}^E=\frac{1}{6}\sum_{2\sigma}^{7}\vec{J}^E_\sigma$, $\vec{J}^E_\sigma$ being the local current in layer σ. In the center-of-mass reference frame the heat current $\vec{J}^Q$ equals the energy current. The thermal conductivity λ may thus be computed via Fourier's law:

$$\vec{J}^Q=-\lambda\vec{\nabla}T\ . \tag{12}$$

The values of λ found in this way are affected by an error which is given by the combined errors on $\vec{J}^Q$ and $\vec{\nabla}T$:

$$\frac{\Delta\lambda}{\lambda}=\frac{\Delta J^Q}{J^Q}+\frac{\Delta(\nabla T)}{\nabla T}\ .$$

$\Delta J^Q=\sigma(J^E_\sigma)/\sqrt{6}$, where σ is the standard deviation of the layer's current J^E_σ and

$$\frac{\Delta(\nabla T)}{\nabla T}=\frac{1}{r}\left[\frac{1-r^2}{4}\right]^{1/2},$$

where r is the correlation coefficient.[11]

In Fig. 6 are reported the values of λ computed at the density $\rho=0.75$ with time averages of 5000 steps. The result of one simulation is not reported because in that case the signal-to-noise ratio was nearly 1, the signal being the heat current in the

direction parallel to the thermal gradient and the noise being the heat current in the directions perpendicular to the thermal gradient. The values of λ reported have been obtained by imposing the gradients to initial states with three different temperatures. The expected variation of λ with the temperature in that range[9] is indicated by the error bar on the λ axis and is much smaller than the scattering of the λ values; therefore no dependence of λ on T could be checked within the precision of our computations. As for the dependence of λ on ∇T, no definite trend may be observed so that it must be assumed that the highest gradients are still in the region of linear thermal response.

In Fig. 6 we have also reported the values of λ obtained by Ashurst[2] by a different nonequilibrium MD method at a similar density ($\rho=0.761$) and temperature ($T=0.872$). The comparison with our results and with the experimental data show that the precision of the two simulations is similar and confirms that no trend can be detected in the dependence of λ on ∇T.

In Fig. 7 we have reported the values of λ computed at the density $\rho=0.85$ with time averages varying between 4000 and 7000 steps. Here all simulations start from the same initial state and the final temperatures, that is the central values of the linear profiles through the six inner layers are scattered in a narrow range around the initial T. The experimental value of λ corresponding[9] to this temperature is indicated by the horizontal dashed line. The values of λ found by Ashurst[2] at $\rho=0.853$, $T=0.701$ and $\rho=0.844$, $T=0.722$ with

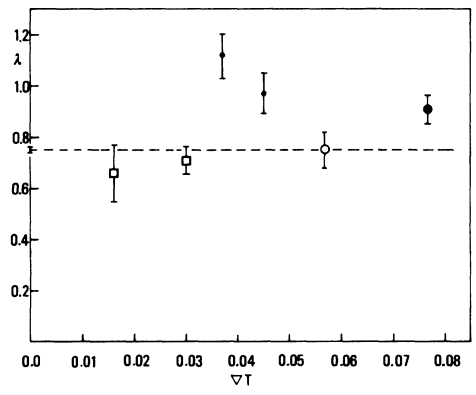

FIG. 6. Thermal conductivity λ as a function of the thermal gradient. $\rho=0.75$: (·) $T=0.909$, (○) $T=1.085$ (and $N=864$), (●) $T=1.296$. (□) data taken from Ref. 2: $\rho=0.761$, $T=0.872$. The dashed line is drawn in the center of the range of experimental values.

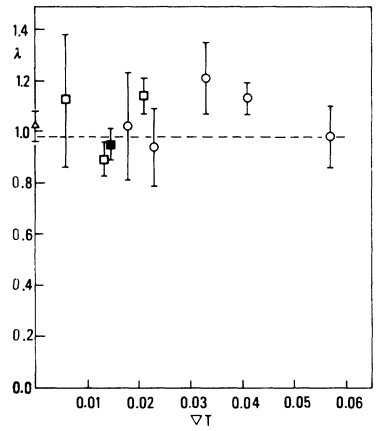

FIG. 7. Thermal conductivity λ as a function of the thermal gradient. (○) $\rho=0.85$, $T=0.801$. Data taken from Ref. 2: (□) $\rho=0.853$, $T=0.701$; (■) $\rho=0.844$, $T=0.722$. (△) Datum from Ref. 3 at $\rho=0.844$, $T=0.715$. The dashed line is drawn at the experimental value.

low gradients are reported for comparison together with the value found by Levesque[3] at $\rho=0.844$, $T=0.722$ via equilibrium Kubo formulas.

The computed values of λ are all scattered around the experimental value for all gradients and do not show any systematic deviation, as in the previous case. Therefore, here too it must be argued that the higher gradients are still in the region of linear thermal response.

In Fig. 8 we have reported the values of λ computed at the average density $\rho=1.113$ with time averages varying between 2000 and 3000 time steps. The points are disposed between 1.5 and 2.0, and it is not possible to see a definite dependence of λ on ∇T.

Here there are no experimental data available for a comparison. However, at density $\rho=1.113$ and $T=2.74$ (on the freezing line) Ashurst[2] has found a value of 2.68 ± 0.20, simulating a gradient $T=0.047$. Similar values for λ have been found by Levesque[3] at the same density: for $T=2.736$, $\lambda=2.60\pm0.15$; for $T=2.803$, $\lambda=2.32\pm0.08$.

The apparent discrepancy between our values and the others must be ascribed to the observed lowering of the bulk density with respect to the average one. It is known that the thermal conductivity depends strongly on the density, increasing monotonically at fixed temperature. In our case the effective bulk density over the six inner layers is $\rho=1.063$ for all gradients simulated at the total density $\rho=1.113$. It is therefore necessary to esti-

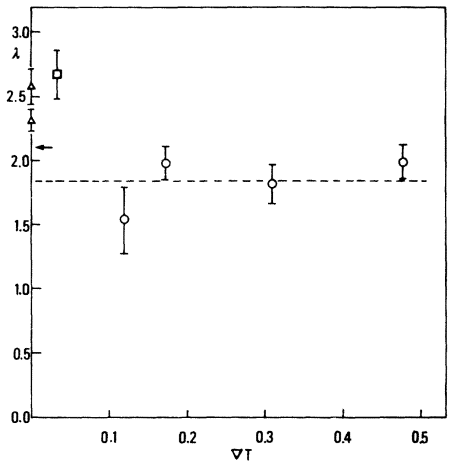

FIG. 8. Thermal conducivity λ as a function of thermal gradient. (○) $\rho=1.063$, $T=2.720$. (□) Datum from Ref. 2 at $\rho=1.113$ and $T=2.74$. (△) Data from Ref. 3 at $\rho=1.113$, $T=2.736$, and $T=2.803$. The arrow indicates the value found via formulas (13) and (14) for $\rho=1.113$ and $T=2.74$. The dashed line is drawn at the value found by formulas (13) and (14) at the effective bulk density $\rho=1.063$ and average temperature $T=2.72$.

mate the expected variation of λ due to this decreased density.

It has been shown that the experimental data for the thermal conductivity in a large range can be expressed as $\lambda=\lambda_0+\lambda_e$, where λ_0 is the thermal conductivity based on dilute gas theory and λ_e is the excess thermal conductivity. λ_0 depends only on the temperature and is given by[12] (in reduced units)

$$\lambda_0=A\sqrt{T}/[1+(B/T)10^{-C/T}], \tag{13}$$

where $A=0.128$, $B=1.276$, and $C=0.050$. In argon, for pressure up to $P=2.5$ and for temperatures between 0.75 and 2.92, λ_e depends only on density; the experimental data are reproduced within 3% by the formula[12]

$$\lambda=\lambda_0+0.113[\exp(0.833\rho/\rho_c)-1], \tag{14}$$

where ρ_c is the critical density ($\rho_c=0.319$).[13] It is questionable if the formula (14) still holds at the very high pressure ($P\simeq 22$) that we find in our simulation. If we use formulas (13) and (14) to estimate λ at $T=2.74$ and $\rho=1.113$, we find $\lambda=2.10$; this extrapolated value seems to underestimate by about 15% the middle point of the values found by Ashurst and Levesque. At our effective bulk density $\rho=1.063$ and $T=2.720$ the same formulas give the value $\lambda=1.85$. The line drawn at this value in Fig. 8 crosses at mid height the range of our thermal conductivity values; even supposing that $\lambda=1.85$ underestimates the true value at our bulk density, this result indicates that within the precision of our simulation our results are consistent with the expected value. Therefore we may conclude that here too there is no systematic deviation from the Fourier's law up to a gradient $\nabla T\simeq 0.5$.

VI. CONCLUSIONS

We have developed a technique based on stochastic thermal walls to produce stationary nonequilibrium thermal states in a molecular dynamics system. The relaxation times involved in the heat exchange between system and heat reservoir are of the order of 10^{-11} sec, thus making the technique suitable for computer experiments. Moreover, we were able to perform an analysis of the local thermodynamical properties by dividing the MD system in layers with thickness of the order of the interatomic distance. We have applied this technique to study the bulk properties in a thermal gradient and to give a physical description of the heat transmission in the region near the thermal wall.

We have simulated high gradients in a region of dense fluids ranging from the gas-liquid coexistence line to the freezing line to check the validity of the linear thermal response (Fourier's law). We have not found any systematic deviation from that law for gradients up to $\nabla T\simeq 0.08$ at $\rho=0.75$, $\nabla T\simeq 0.06$ at $\rho=0.85$, and $\nabla T\simeq 0.5$ at $\rho=1.063$. The last gradient corresponds to 1.8×10^9 K/cm for argon.

Our technique implies a surface effect of the boundary conditions on the local density; this effect is relevant only at the highest density, when the compressibility factor is much greater than one. In the bulk, where this effect is absent, we found that local equilibrium holds over a region with linear dimension of the order of σ ($\sigma\sim 3.4$ Å for argon).

Work is in progress to extend our method to shear flow and to reduce the mentioned effect of our boundary conditions.

ACKNOWLEDGMENTS

We are greatly indebted with D. Levesque and J.-J. Weis for useful discussions and for kindly

providing unpublished data on the equation of state and thermal conductivity. We thank G. Jacucci for suggestions on the heat transmission effect and Y. Adda for stimulating support. Finally, we are pleased to acknowledge the warm hospitality by C. Moser at CECAM where an essential part of this work has been done.

---

[1]G. Ciccotti and A. Tenenbaum, J. Stat. Phys. 23, 767 (1980).

[2]W. T. Ashurst, paper presented at the 13th International Conference on Thermal Conductivity, Lake Orzak, Missouri, Nov 5—7, 1973, in *Advances in Thermal Conductivity* (University of Missouri-Rolla, Rolla, Missouri, 1976), p. 89.

[3]D. Levesque, L. Verlet, and J. Kürkijarvi, Phys. Rev. A 7, 1690 (1973); and D. Levesque (unpublished results). In the latters the result for the thermal conductivity given in the published paper has been corrected.

[4]L. Verlet, Phys. Rev. 159, 98 (1967).

[5]J. L. Lebowitz and H. Spohn, J. Stat. Phys. 19, 633 (1978).

[6]S. Goldstein, J. L. Lebowitz, and E. Presutti, colloquium on Random Fields: Rigorous Results in Statistical Mechanics and Quantum Field Theory, Hungary, June, 1979 (unpublished).

[7]J. H. Irving and J. G. Kirkwood, J. Chem. Phys. 18, 817 (1950).

[8]See, for example, H. Ziebland, in *Thermal Conductivity*, edited by R. P. Tye (Academic, New York, 1969), Vol. 2.

[9]*Gas Encyclopaedia* (Elsevier, Amsterdam, 1976).

[10]L. Verlet and J.-J. Weis, Phys. Rev. A 5, 939 (1972). The data to which we refer in the text have been kindly supplied by J.-J. Weis.

[11]J. E. Freund, *Mathematical Statistics* (Prentice Hall, Englewood Cliffs, N.J., 1962), Chap. 13.

[12]B. J. Bailey and K. Kellner, Physica 39, 444 (1968).

[13]A. Michels, J. M. Levelt, and W. De Graaff, Physica 24, 659 (1958).